

Reinforcement Learning Based Bidding Framework with High-dimensional Bids in Power Markets

Jinyu Liu, *Student Member, IEEE*, Hongye Guo, *Member, IEEE*, Yun Li, Qinghu Tang, *Student Member, IEEE*, Fuquan Huang, Tunan Chen, Haiwang Zhong, *Senior Member, IEEE* and Qixin Chen, *Senior Member, IEEE*

Abstract—Over the past decade, bidding in power markets has attracted widespread attention. Reinforcement Learning (RL) has been widely used for power market bidding as a powerful AI tool to make decisions under real-world uncertainties. However, current RL methods mostly employ low dimensional bids, which significantly diverge from the N price-power pairs commonly used in the current power markets. The N -pair bidding format is denoted as High Dimensional Bids (HDBs), which has not been fully integrated into the existing RL-based bidding methods. The loss of flexibility in current RL bidding methods could greatly limit the bidding profits and make it difficult to tackle the rising uncertainties brought by renewable energy generations. In this paper, we intend to propose a framework to fully utilize HDBs for RL-based bidding methods. First, we employ a special type of neural network called Neural Network Supply Functions (NNSFs) to generate HDBs in the form of N price-power pairs. Second, we embed the NNSF into a Markov Decision Process (MDP) to make it compatible with most existing RL methods. Finally, experiments on Energy Storage Systems (ESSs) in the PJM Real-Time (RT) power market show that the proposed bidding method with HDBs can significantly improve bidding flexibility, thereby improving the profit of the state-of-the-art RL bidding methods.

Index Terms—Power market , energy management , reinforcement learning , high-dimensional bids.

I. INTRODUCTION

MARKET uncertainty is becoming a crucial aspect of power market bidding.[1] In recent years, the variability in power generation has led to more fluctuating day-ahead (DA) and real-time (RT) market prices[2]. The increase in market price uncertainty poses a greater challenge for market bidding.

This trend of rising uncertainty is expected to persist in the following decades due to the increase in renewable generations[3]. The International Renewable Energy Agency (IRENA) has projected that the worldwide installed capacity of renewable energy sources will increase significantly in the coming years. Currently, renewables account for approximately 30% of the total generation capacity. This figure is projected to surpass 50% by 2035[4]. The future power system will be more reliant on renewables, and the power markets will face higher uncertainties.

This work was supported in part by the Science and Technology Project of China Southern Power Grid under Grant 090008KC23020006

Jinyu Liu, Hongye Guo (Corresponding Author, e-mail: hyguo@mail.tsinghua.edu.cn), Qinghu Tang, Haiwang Zhong, and Qixin Chen are with the State Key Laboratory of Power Systems, Department of Electrical Engineering, Tsinghua University, Beijing 100084, China.

Yun Li, Fuquan Huang, and Tunan Chen are with the Shenzhen Power Supply Co. Ltd., Shenzhen 518001, China. Tunan Chen is also with the Tsinghua Shenzhen International Graduate School, Shenzhen 518071, China.

To achieve high profits under high market uncertainties, generation companies (GENCOs) must wisely strategize their market bids to ensure market profits. The topic of strategic bidding has been a hotspot of research for the last decade. To tackle the rising uncertainties in power markets, RL-based methods have been widely adopted to tackle the real-world market uncertainties.

RL is a subset of Machine Learning (ML), focusing on training algorithms to make a sequence of decisions by interacting with an environment to achieve a goal, where success is measured by a system of rewards and penalties.

Past RL-based bidding methods have been applied to multiple-market[5] and multiple-subject[6] bidding scenarios, both under real-world uncertainties. Although RL-based bidding methods can address real-world uncertainties, they have a fundamental drawback: they cannot effectively utilize HDBs in bidding.

The HDB is the most common bid format in real-world power markets. An HDB consists of several price-power pairs arranged in monotonic increasing order[7]. GENCOs use these bidding pairs to indicate how much power they are willing to commit to a certain market price, especially when the price is highly volatile. In the PJM[7], CAISO[8]and AEMO[9] power market, N equals 10, which means 10 dimensions are used to represent bidding prices, and another 10 dimensions are used to represent bidding quantities. Because these bidding pairs are formulated in a high-dimensional space ($2N$ is usually 20), we refer to this real-world bid format as the High-Dimensional Bids (HDBs) in this paper, compared with the Low-Dimensional Bids (LDBs) used in most current studies.

The HDBs in bidding strategies are important for GENCOs to cope with the rising price uncertainty. As prices are hard to predict very accurately in certain real-world markets[10, 11], it is difficult for GENCOs to schedule the generation plan beforehand, especially for new-type market participants such as Energy Storage System (ESS) and Virtual Power Plant (VPP). In this case, GENCOs can use HDBs to indicate their generation plan for N in different market price ranges. So that they can achieve a satisfactory market clearing result at every market clearing price. The HDB is a useful tool to express GENCOs' willingness on the market prices in the market clearing process.

Currently, HDBs (High-dimensional Bids) are mostly considered by optimization-based approaches, but rarely utilized in RL-based methods. Optimization-based methods are able to utilize HDB's high dimensionality by optimizing the bid parameters by modeling the possible market outcomes.

They mostly utilize stochastic programming[12, 13]and robust programming[14, 15] to optimize the bid parameters. Because optimization-based methods can fully utilize the known models for bidding, they are outstanding for market scenarios that can be completely modeled. However, many optimization-based methods[12, 13, 14] rely on price predictions to schedule the generator in the real world, so the precision of price predictions will obviously affect the effectiveness of the bidding strategies. The performance of optimization-based methods bidding has been surpassed by RL-based methods in high-uncertainty scenarios [16, 17], including the real-time market ESS bidding studied in this paper [17]. Because the price forecast accuracy is low in such a case[10, 11], it is difficult for optimization-based methods to bid effectively.

RL-based methods can tackle real-world uncertainties by learning real-world market data, but they currently can only utilize Low-Dimensional Bids (LDBs), like one-value price bids[6, 17, 18], one-value power bids[19, 20, 21], one-pair price-power bids[16, 22, 23] etc. These LDBs are all greatly simplified versions of HDBs. For example, [17]-[18] use a bidding format of one price bid with fixed power, and the clearing result is either zero power or full power. [19]-[21] use one-power bids, which means they decide their power output regardless of actual market prices. [16]-[23] use the bid format of one price-power pair, where the GENCO submits a price threshold for generating power, and a power quantity to indicate how much power it is willing to generate. Such LDBs are greatly simplified from the HDBs in real-world power markets. The loss of flexibility in market bids can cause loss in the bidding performance[12, 13].

Though these bidding formats are easier to learn using RL-based methods, they sacrifice the expressiveness of the market bids. They only have 0~2 price/power bids, and cannot fully reflect the GENCOs' willingness on the market prices.

There have been a few RL-based bidding methods that have attempted to adopt the HDB format[24, 25, 26, 27], but usually in an indirect way. In detail, they fail to generate HDBs in the original high-dimensional and continuous HDB space, which ignores the most important features of HDB format in bidding. Instead, these methods use case-specific simplifications to transform the high-dimensional bidding space into low-dimensional spaces, which inevitably hurts the degree of freedom of bids. For example, [24, 28] use the overflow proportion as a low-dimensional continuous bidding space, where they decide the overflow ratio of the actual thermal generator cost curve. [25] assumes that the HDBs are in the space of an affine function and decides the slope of this affine bidding function. [26] make decisions in a discrete space consisting of nine HDB samples and convert the bidding problem to a nine-option decision problem.[27] designs a custom set of decision variables and converts the bidding space to a 3-dimensional continuous space.

These methods utilize HDBs in an indirect way and have the following defects: First, they cannot make decisions in the original HDB space and cannot fully utilize the potential of HDBs. Second, they require specific parameterization designs for specific bidding problems, which may hinder their ability to adapt to new entities and market conditions. Third, because

the parameterization designs are manually specified, they could be suboptimal and limit the bidding performances.

To overcome the above-mentioned challenges, this paper intends to propose an HDB generation framework for RL-based methods. The proposed framework can serve as a tool for various types of bidding entities to better utilize HDBs for market bidding in real world. However, several challenges are involved in achieving the above aims. Firstly, we need to generate HDBs that are suitable for RL-based bidding methods. This includes encoding the bids in a format that captures the essential information needed for decision-making in the bidding process while ensuring that the representation is compact enough to facilitate quick learning and actioning by the RL model. Secondly, we need to ensure that the generated HDB satisfies market bidding requirements, such as bidding pairs' monotonicity of HDBs. This ensures that the final bidding strategy is not only optimized for profitability or cost-effectiveness but also complies with market rules and expectations. Thirdly, the proposed framework should be adaptable to different fuel types and RL methods so that it can be tailored to meet a wide range of requirements and scenarios in the energy market bidding landscape. To the best of our knowledge, there has not been an RL-based bidding algorithm that can generate the HDBs without simplification.

In this paper, we propose an HDB generation framework that is compatible with most RL algorithms. It supports efficient and effective HDB bidding under high uncertainties. First, we identify a special type of neural network with price input and power output, which is called the Neural Network Supply Function (NNSF). Second, we extract HDBs from the NNSFs' input-output relationship. The extracted HDBs will satisfy the market bidding requirements, and will keep the essential bidding strategy of the NNSF. Third, we approximate the HDB bidding process with NNSF and use the approximation to propose a training process that is suitable for most RL training frameworks. Finally, we conduct experiments on Energy Storage Systems (ESSs) in real-world power market, such as PJM. We demonstrate that the proposed HDB generation method can improve the bidding performance of the state-of-the-art RL-based bidding methods.

The main contributions of this paper are summarized as follows:

- A neural network based modeling method for HDB bidding has been proposed, which exhibits three key characteristics: it achieves lossless representation of HDBs, meets the feature requirements of real market bids, and facilitates integration into RL for training.
- This paper proposes a framework that combines HDB with RL methods. It includes the training and testing phases. This framework is compatible with the majority of RL methods and facilitates improvements in HDB biddings.
- The proposed method's effectiveness is shown in Energy Storage Systems (ESS) in the real-world PJM RT power market. The proposed HDB bidding algorithm can significantly improve bidding flexibility and improve bidding arbitrage performance by 15.40% compared with the RL-based bidding methods that utilize LDBs.

The rest of this paper is organized as follows. In Section II, we describe the bidding problems. In Section III, we generate HDBs from the input-output relationship of NNSFs. In Section IV, we learn NNSF with RL algorithms. In Section V, we conduct performance evaluations. Finally, conclusions are made in Section VI.

II. SYSTEM MODEL AND PROBLEM FORMULATION

In this paper, we consider an ESS that uses HDBs to participate in the real-world RT energy market. First, we will describe the HDB clearing model and the ESS model, then formulate the HDB bidding problem of the RT energy market.

A. HDB based Market Bidding Model

An HDB consists of a series of N price-power pairs that increase in a monotonically ascending manner. We denote HDBs with the price bids, denoted as $\bar{\lambda}_i$, and the power bids, denoted as \bar{p}_i . The HDB needs to satisfy the following constraints:

$$\begin{aligned} \lambda_{\min} &\leq \bar{\lambda}_i \leq \lambda_{\max} \\ p_{\min} &\leq \bar{p}_i \leq p_{\max}, \text{ for } i = 1, \dots, N \\ \bar{\lambda}_i &\leq \bar{\lambda}_{i+1} \\ \bar{p}_i &\leq \bar{p}_{i+1}, \text{ for } i = 1, \dots, N \end{aligned} \quad (1)$$

A market bidding pair $(\bar{\lambda}_i, \bar{p}_i)$ is accepted by the power market if its bidding price is lower than the market clearing price. The power of the largest accepted bidding pair will be the market clearing power of the bidder.

In power markets, one HDB could be cleared for multiple rounds. For example, in the RT energy market, an HDB is submitted hourly, and the market clearing is conducted for the next 12×5 minutes. Therefore, all HDB values can affect the clearing results of a period.

B. ESS Model

In this subsection, we propose the ESS model based on lithium-ion batteries. With the significant decrease in battery production costs, batteries can now economically power major energy shifts. The ESS participates in the RT energy market, which is one of the most profitable energy markets for energy arbitrage. The proposed ESS model considers its state transition and its bidding objective.

The internal state of an ESS is changed according to the State of Charge (SoC) model. It can be described in time-step formats:

$$\begin{aligned} SoC_t &= SoC_{t-1} + \tau(\eta^c p_t^c - \frac{p_t^d}{\eta^d}) \\ 0 &\leq SoC_t \leq SoC_{\max}, \\ 0 &\leq p_t^c \leq p_{\max}, \\ 0 &\leq p_t^d \leq p_{\max}, \\ p_t^c \cdot p_t^d &= 0 \end{aligned} \quad (2)$$

where τ is the timestep, usually 5 minutes for the RT market. η^c, η^d represents the charging and discharging efficiency

of the ESS, and p_t^c, p_t^d are the charging and discharging power. p_t^c and p_t^d cannot be non-zero at the same time.

The bidding objective of an ESS consists of three parts, including the market bidding income, the ESS depreciation cost, and the SoC penalty rewards:

$$r_t = \sum_t \lambda_t \cdot p_t^d + \sum_t r_t^{dep} + \sum_t r_t^{soc_violate} \quad (3)$$

The first term is the market bidding income based on clearing results of (1), where λ_t is the energy market clearing price. The second term is the ESS's depreciation costs. Since the modeling of ESS is not the focus of this paper, we consider a typical degradation cost that is proportional to the discharge power and time elapsed[29]. The cost model can be expressed formally as:

$$r_t^{dep} = -\lambda^{dep} \cdot p_t^d \cdot \tau \quad (4)$$

where λ^{dep} is the depreciation cost constant. The negative sign means the reward for depreciation is always negative.

The third term is the SoC violation penalty of the ESS. In the RL training process, the RL actor's actions could lead to an invalid SoC. In such cases, an additional penalty is added to the RL training process to avoid SoC violations. The SoC violation penalty can be expressed as:

$$r_t^{soc_violate} = \begin{cases} 0 & , 0 \leq SoC_{t+1} \leq SoC_{\max} \\ -P & , \text{ else} \end{cases} \quad (5)$$

where P is the reward penalty constant.

C. Bidding Problem Formulation

Next, to solve the bidding problem with RL, we will describe the bidding problems of the ESS using Markov Decision Processes (MDPs). The MDP is a mathematical framework used to model decision processes where outcomes are influenced by both randomness and the decisions made by the decision-maker. An MDP is defined by a tuple $(\mathcal{S}, \mathcal{A}, \mathcal{R}, \mathcal{T}, \gamma)$, consisting of state, action, reward, transitions, and discount factor. At each time step, the agent observes the current state of the environment $s_t \in \mathcal{S}$ and takes an action $a_t \in \mathcal{A}$. The environment transitions to a new state s_{t+1} by transition \mathcal{T} , and the agent receives a reward signal $r_t(s_t, a_t) \in \mathcal{R}$ that indicates the desirability of the state-action pair. The goal of the agent is to learn a policy π , which is a mapping from state to actions, that maximizes the cumulative reward $\sum_{t=1}^{\infty} \gamma^t r_t(s_t, a_t)$ over time. The discount factor γ is between 0 and 1, which measures the importance of future rewards and instant rewards. The ESS bidding MDP is formulated as follows. It has a state \hat{s}_t , which consists of market observation and energy levels by the bid submission time. (We use \hat{s}_t instead of s_t because the state will be augmented later) The action a_t is the HDB (1), which is the output of the bidding policy. The reward r_t is the bidding objective (3). The transition probability \mathcal{T} consists of two parts. The first part is the ESS's energy level transitions (2). The second part is the market price transition, which is influenced by multiple market factors. Because the second part of the transition probability

is complicated and hard to model, we will not formulate it explicitly. Instead, we use real-world data of this transition probability, which are the real-world market price histories to simulate the transition. A certain portion of historical prices are used to simulate the training set, and a certain portion of more recent prices are used to simulate the testing set.

The bidding objective is to maximize the total reward (3) with the HDBs (1).

III. NEURAL NETWORK BASED HDB GENERATION

In this section, we propose an HDB generation framework that generates HDB actions from market states by employing a special type of neural network called NNSF. The generated HDBs will satisfy the HDB bidding rules (1) and can be submitted for market bidding. The HDB generation framework further enables neural network training with RL of Section IV.

The proposed framework to generate HDBs from neural networks is shown in Fig. 1. First, a supply curve is sampled from the NNSF's input-output relationship in the *Supply Curve Sampling* process. In this process, the NNSF's output is sampled multiple times with different input prices (from λ_{\min} to λ_{\max} with step size $\delta\lambda$). The corresponding price-power pairs constitute the supply curve. Second, a $2N$ dimensional HDB is extracted from the supply curve in the *HDB Extraction* process. Three steps are introduced to extract an HDB from the supply curve, which are the monotonize, discretize, and output steps. The extracted HDB will satisfy the bidding rule (1). Third, the HDB is submitted to market clearing, and the market operator computes the clearing price and clearing power result and returns the bidding reward. Finally, we proceed to the next bidding step.

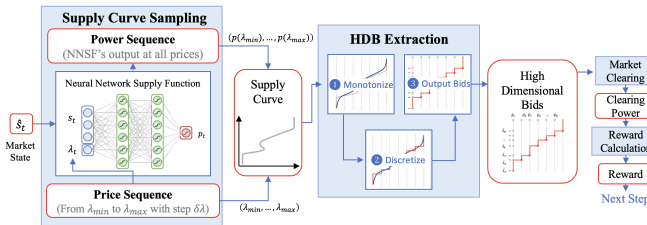


Fig. 1. The proposed HDB generation framework

The main idea of the proposed HDB generation framework can be understood as follows. An infinite dimensional HDB (when $N \rightarrow \infty$) is a continuous supply curve, which continuously maps price to power. We use a continuous function (the NNSF) to represent the supply curve so that it can be improved by neural network training (Section IV). Because the $2N$ -dimensional HDBs are downsampled from infinite-dimensional supply curves, the $2N$ -dimension flexibility can be utilized. Past methods can achieve bidding flexibility of a maximum 4-dimension[22], and the proposed method can achieve $2N$ -dimension so that the bidding flexibility is significantly improved.

In this section, we will first introduce the NNSF in Section III-A. Then, we propose the supply curve sampling process in Section III-B and the HDB extraction process in Section III-C. At last, the suitability of the proposed

HDB generation framework to RL algorithms is discussed in Section III-E.

A. Neural Network Supply Function

In this paper, we use a special class of neural networks to generate supply curves, which we name the NNSF.

In economics, the supply curve (or supply function) is a fundamental concept that represents the relationship between the quantity of a good or service that producers are willing and able to sell and its price.

In machine learning, neural networks can be used to represent any arbitrary function and neural networks are used as versatile function approximators. Therefore, they can be used to represent the supply curves (the supply function) of a bidder.

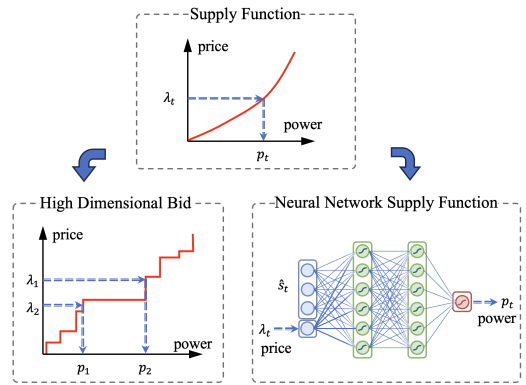


Fig. 2. HDB and NNSF are both Supply Functions

Using these observations, we define neural networks that have price inputs and power outputs as NNSFs. By definition, an NNSF maps price to power, and the mapping is a neural network. Additionally, the shape of the supply curve is also determined by various factors, such as the ESS state, the time of bidding, the market price trend, etc. Therefore, NNSF has an additional input of market state \hat{s}_t .

In the following context, we will denote the NNSF as $p_t = \pi_\theta(\hat{s}_t, \lambda_t)$, where π is the neural network, θ is the neural network parameter, \hat{s}_t is the market state input, and λ_t is the market price input. \hat{s}_t and λ_t consist of the full input (full state) s_t of the NNSF. The output of the NNSF is the output power p_t .

B. Supply Curve Sampling

The first step of generating HDBs is sampling a supply curve from the NNSF. The supply curve ($\lambda - p$) is the NNSF's input-output relationship at a certain market state input \hat{s}_t . The supply curve is a point set consisting of M price-power pairs. The schematic of the supply curve sampling process is shown in Fig. 1.

The supply curve is derived by sampling the neural network's output value across the whole price range. The price range $[\lambda_{\min}, \lambda_{\max}]$ is divided into M segments with step size $\delta\lambda$. The NNSF's power output at each segment is computed: $p_{(\cdot)} = \pi_\theta(\hat{s}_t, \lambda_{(\cdot)})$. Finally, the

NNSF's price-power relation is sampled as the supply curve: $[(\lambda_{\min}, \dots, \lambda_{\max}), (p(\lambda_{\min}), \dots, p(\lambda_{\max}))]$.

Note that the supply curve sampling process can be computed in parallel, avoiding $\mathcal{O}(M)$ time complexity. Since neural networks are typically deployed on GPUs designed for parallel computations, the network sampling operation can use a batch size of M . If the GPU computes the entire batch in parallel, the computation time complexity is $\mathcal{O}(1)$. In our experiments, we will demonstrate that this process is computationally efficient.

C. HDB Extraction

In this subsection, we will extract HDBs from the supply curves.

The supply curve and the HDB are both supply functions. However, HDBs are supply functions that have special requirements. To be specific, HDBs are *monotonic* and *discrete-output* supply functions. The HDB bidding rule (1) defines a special family of supply functions. First, the supply function should be *monotonic*, so that the bidding power increases with the market price. Also, the supply function should have N *discrete* outputs so that the bidding power can be expressed with the N -dimensional power bids.

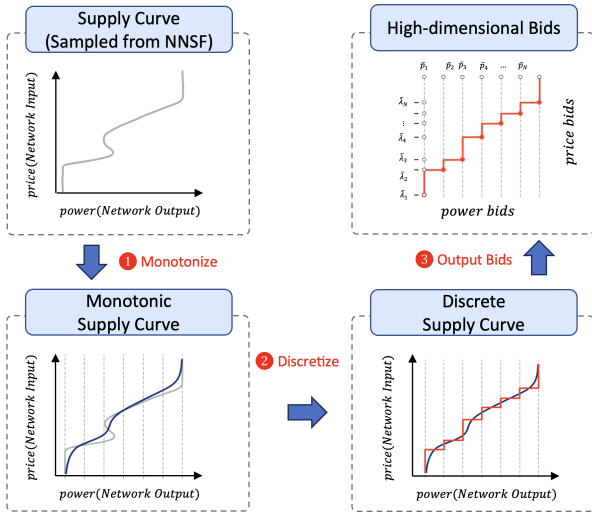


Fig. 3. Represent the high-dimensional bids with monotonic and discrete-output neural networks

As shown in Fig. 3. We propose a three-step process to generate HDBs from supply curves. First, we need to monotonicize the supply curve so that the supply curve satisfies the monotonicity requirement. Second, we need to discretize the network output values so that the supply curve satisfies the discrete-output requirement. Finally, because the monotonicized and discretized neural network uniquely corresponds to an HDB, the HDB parameters can be extracted. Next, we will implement an algorithm to realize the HDB extraction process.

In the following contexts, we define the parameters of HDBs by price-power anchor points: $[\bar{\lambda}_i, \bar{p}_i]$, where $i = 1, \dots, N$. According to the HDB rule (1), the bid price and bid power should be monotonically increasing: $\bar{\lambda}_i \leq \bar{\lambda}_{i+1}, \bar{p}_i \leq \bar{p}_{i+1}$.

We will shorthand the NNSF as $p = \pi(\lambda)$ to show its nature as a supply function. We will denote the supply curve as (λ_k, p_k) , where $k = 1, \dots, M$, to show its nature as a point set. Note that $p_k = \pi(\lambda_k)$.

The HDB extraction problem is to approximate the supply curve (λ_k, p_k) with $[\bar{\lambda}_i, \bar{p}_i]$ with low approximation errors.

The first step is to monotonicize the supply curve. In the experiment sections, we will show that the supply curves can be considered naturally monotonic in most cases. Therefore, the monotonic step is not necessary most of the time. For the non-monotonic cases, we use a simple method to monotonicize the supply curve: The sampled supply curve points are valued as the cumulative max: $p_k \leftarrow \max\{p_1, p_2, \dots, p_k\}, \forall k = [1, M]$. So that $p_{k-1} \leq p_k$, and the supply curve is monotonic.

The second step is to discretize the supply curve. In this step, we find the optimal HDB parameters to approximate the monotonicized supply curve using an iterative algorithm. We define the approximation error as the squared deviation between the original NNSF and the approximated HDB. The approximation error is denoted as e_d . It can be written as the sum of the approximation errors of each HDB segment to the supply curve:

$$e_d = \sum_i \int_{\bar{\lambda}_i}^{\bar{\lambda}_{i+1}} (\pi(\lambda) - \bar{p}_i)^2 d\lambda \quad (6)$$

Then, to minimize the error, we propose an iterative *greedy algorithm*. In each iteration, we find the optimal value of $\bar{\lambda}_i$ and \bar{p}_i given other $\bar{\lambda}_{-i}$ and \bar{p}_{-i} values fixed, where $-i$ means all other indexes except for i . Using optimality conditions, at the optimal $\bar{\lambda}_i$ and \bar{p}_i , the partial derivatives of $\bar{\lambda}_i$ and \bar{p}_i with respect to e_d should be zero:

$$0 = \frac{\partial e_d}{\partial \bar{\lambda}_i} = \frac{\partial}{\partial \bar{\lambda}_i} \left[\int_{\bar{\lambda}_{i-1}}^{\bar{\lambda}_i} (\pi(\lambda) - \bar{p}_{i-1})^2 d\lambda + \int_{\bar{\lambda}_i}^{\bar{\lambda}_{i+1}} (\pi(\lambda) - \bar{p}_i)^2 d\lambda \right] \quad (7)$$

$$= (\pi(\bar{\lambda}_i) - \bar{p}_{i-1})^2 - (\pi(\bar{\lambda}_i) - \bar{p}_i)^2$$

$$0 = \frac{\partial e_d}{\partial \bar{p}_i} = \int_{\bar{\lambda}_i}^{\bar{\lambda}_{i+1}} \frac{\partial}{\partial \bar{p}_i} (\pi(\lambda) - \bar{p}_i)^2 d\lambda \quad (8)$$

$$= 2 \left[\int_{\bar{\lambda}_i}^{\bar{\lambda}_{i+1}} \pi(\lambda) d\lambda - \bar{p}_i (\bar{\lambda}_{i+1} - \bar{\lambda}_i) \right]$$

The optimality conditions can be simplified using the monotonic feature of HDBs to:

$$\begin{cases} \bar{\lambda}_i = \pi^{-1} \left(\frac{1}{2} (\bar{p}_{i-1} + \bar{p}_i) \right) \\ \bar{p}_i = \int_{\bar{\lambda}_i}^{\bar{\lambda}_{i+1}} \pi(\lambda) d\lambda / (\bar{\lambda}_{i+1} - \bar{\lambda}_i) \end{cases} \quad (9)$$

where π^{-1} is the inverse function of π . (9) calculates the optimal $\bar{\lambda}_i$ and \bar{p}_i explicitly. However, because the inverse function and the integration of $\pi(\lambda)$ cannot be precisely calculated, we use supply curves to approximate these two terms so that (9) can be computed.

To compute (9), first, we use the supply curve to approximate the inverse function and the integrations. The inverse

function can be achieved by looking up the value of the supply curve where $p_k = \frac{1}{2}(\bar{p}_{i-1} + \bar{p}_i)$, and returning the corresponding λ_k . If the supply curve samples p_k cannot exactly match $\frac{1}{2}(\bar{p}_{i-1} + \bar{p}_i)$, the closest p_k is chosen. Next, to approximate \bar{p}_i , the formula (9) can be understood as the mean value of $\pi(\lambda)$ in the range $\bar{\lambda}_i$ to $\bar{\lambda}_{i+1}$, which can be approximated with the mean value of $\{p_k\}$ in the range $\bar{\lambda}_i$ to $\bar{\lambda}_{i+1}$. Finally, (9) can be approximately computed as:

$$\begin{cases} \bar{\lambda}_i = \lambda_k, & \text{where } p_k = \frac{1}{2}(\bar{p}_{i-1} + \bar{p}_i) \\ \bar{p}_i = \text{mean}(\{p_k\}), & \text{for all } k : \bar{\lambda}_i \leq \lambda_k < \bar{\lambda}_{i+1} \end{cases} \quad (10)$$

(10) represents the fundamental iterative step of the HDB discretization algorithm. All anchor points $[\bar{\lambda}_i, \bar{p}_i]$ are updated accordingly until convergence.

The output of the final step of (10) will satisfy the requirements of a market HDB. First, because the supply curve is monotonized in the first step, the generated HDBs will satisfy the monotonization requirement. Also, because the output value $\bar{\lambda}_i, \bar{p}_i$ corresponds to the discrete steps of HDBs, the discretization requirement is also satisfied. As a result, $[\bar{\lambda}_i, \bar{p}_i]$ can be extracted and output as the HDB and output as a valid HDB.

D. The proposed HDB generation Algorithm

The pseudo-code of the HDB generation algorithm combining supply curve sampling and HDB extraction is shown in Algorithm 1. The HDB generation precision and computational efficiencies will be discussed in the experiment sections.

Algorithm 1 HDB generation

- 1: **Input:** The NNSF π with trained parameter θ .
- 2: **Output:** High-dimensional Bids: $\{(\lambda_t^i, p_t^i)\}$
- 3: **for** $t = 1, 2, \dots, T$ **do** \triangleright For T periods that requires HDB generation.
- 4: Get the market observation $\{\hat{s}_t\}$.
- # Supply Curve Sampling
- 5: Compose the full observaion with price ranges (\hat{s}_t, λ_k) for $\lambda_k = \lambda_{\min}, \dots, \lambda_{\max}$ with stepsize $\delta\lambda$.
- 6: Parallely Sample the NNSF by $p_k = \pi_\theta(s_t, \lambda_k)$ for supply function point set (λ_k, p_k)
- # HDB Extraction
- 7: $p_i \leftarrow \max\{p_1, p_2, \dots, p_i\}$ \triangleright a. Monotonize
- 8: Initialize $(\bar{\lambda}_i, \bar{p}_i), i \in \{1, 2, \dots, P\}$ \triangleright b. Discretize
- 9: $(\bar{\lambda}_0, \bar{p}_0) \leftarrow (\lambda_{\min}, p_{\min})$
- 10: $(\bar{\lambda}_{P+1}, \bar{p}_{P+1}) \leftarrow (\lambda_{\max}, p_{\max})$
- 11: **while** not converge **do**
- 12: **for** $i \in \{1, 2, \dots, P\}$ **do**
- 13: Update each pair $(\bar{\lambda}_i, \bar{p}_i)$ according to:

$$\begin{cases} \bar{\lambda}_i = \lambda_k, & \text{where } p_k = \frac{1}{2}(\bar{p}_{i-1} + \bar{p}_i) \\ \bar{p}_i = \text{mean}(\{p_k\}), & \text{for all } k : \bar{\lambda}_i \leq \lambda_k < \bar{\lambda}_{i+1} \end{cases}$$
- 14: **end for**
- 15: **end while**
- 16: Store the HDB: $(\bar{\lambda}_i, \bar{p}_i), i = 1, \dots, N$ as $\{(\lambda_t^i, p_t^i)\}$ \triangleright c. Output Bids
- 17: **end for**

E. Discussion: the Difficulty of Applying RL to the HDB generation framework

Note that, even though the proposed HDB generation framework(Fig. 1) is able to generate HDBs from NNSFs, it can hardly be used to train an NNSF neural network with RL.

The main reason is that the HDB generation framework does not follow the typical state-action-reward structure in RL. Instead, it is a state-multiple_actions-reward structure. To be specific, because the final bid (the submitted HDB) is extracted from the NNSF's output across the whole price range, the NNSF is forwarded M times (usually M is hundreds of times to generate a supply curve). Because one reward corresponds to hundreds of actions, it is impractical to optimize the NNSF with such an action-reward ratio.

To tackle this problem, in the next section, we will approximate the HDB generation framework to be more RL-friendly and propose an RL-based NNSF training algorithm. Further, we will demonstrate the effectiveness of the proposed approximation in the experiments.

IV. RL-BASED NNSF TRAINING

In this section, we will propose an approximation of the HDB generation framework (Fig. 1) and use the approximation to train NNSFs with RL algorithms (Section IV-B). Finally, a refinement of the NNSF output space is proposed for ESS bidding in Section IV-C.

A. Simplified Bidding Framework for RL

In this subsection, we first simplify the HDB generation framework by approximating the market clearing result with NNSF's output. Then, we propose a more RL-friendly bidding process that is equivalent to HDB bidding. It will follow the typical state-action-reward RL structure.

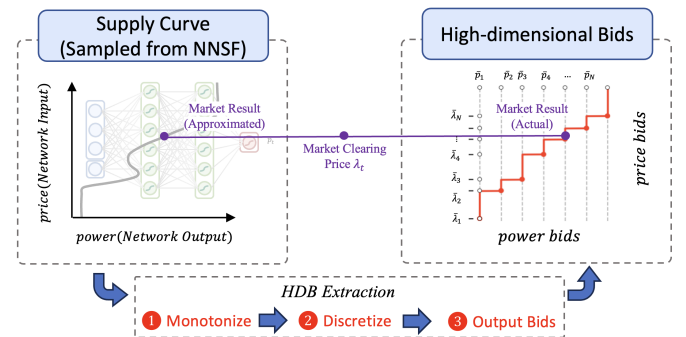


Fig. 4. Approximate the market clearing result with NNSF's output at the market clearing price

Fig. 4 shows how market clearing results can be approximated with the NNSF's output at the market clearing price. Recall that the actual market clearing result is a *point sample* on the HDB bidding curve (right purple dot). It is the HDB supply function's value at the market clearing price. Because the HDB supply function is an approximation of the supply curve. The market clearing power can be approximated with the supply curve's value at the market clearing price.

In other words, to get the market clearing result, we do not need to formulate the full HDB by supply curve sampling and HDB extraction. Instead, we can approximate the market clearing result by the output of the NNSF at the *actual market clearing price*.

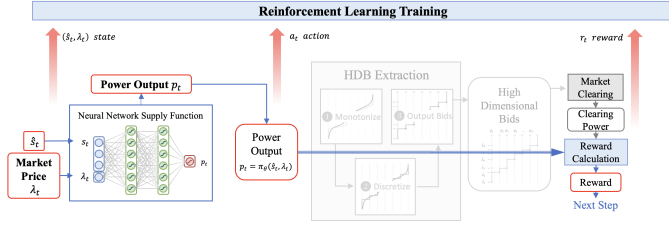


Fig. 5. The proposed NNSF training framework

Leveraging such an approximation, the HDB generation framework (Fig. 1) can be simplified to the NNSF training framework (Fig. 5). In each step, the market state \hat{s}_t and market clearing price λ_t are observed. They are combined to be state $s_t = (\hat{s}_t, \lambda_t)$. s_t is used to sample the NNSF's output of the market clearing price. The output power value denoted as p_t . p_t is considered to be the approximate result of the extracted HDB, and the bidding profit of p_t is computed as the bidding reward. Finally, the bidding history (s_t, a_t, r_t, s_{t+1}) is collected for RL training, and the bidding process proceeds to the next step.

Such a NNSF training framework (Fig. 5) is compatible with RL algorithms. It is a typical state-action-reward MDP. The state is the market information \hat{s}_t and the market clearing price λ_t , the action is the power output p_t , and the reward is the market bidding profit (3).

Note that the training framework has a low-dimensional action space, which is the power output p_t . It transforms the high-dimensional bidding problem into a low-dimensional power dispatch problem. From the perspective of training an RL policy, the proposed RL problem follows the typical state-action-reward structure and can be learned more easily.

Nonetheless, the NNSF training framework does not have the exact same outcome as the HDB generation framework. The NNSF training framework uses the NNSF's output to approximate the HDB generation and market clearing process. It will introduce approximation errors. In the experiments, we will show that such errors can be neglected in practice.

Next, we will propose an RL-based NNSF training algorithm based on the proposed training framework.

B. NNSF Training with the PPO RL Algorithm

This subsection trains the NNSF with the well-known PPO RL algorithm[30]. Other RL algorithms with continuous action spaces are also applicable to our framework. Recall that an RL algorithm improves a policy network by interacting with the environment, and it updates the policy with the interaction history.

We will first introduce the basic principles of RL and the PPO RL algorithm. The PPO algorithm is an actor-critic style RL algorithm. Actor-critic style RL algorithms learn a policy

function $\pi_\theta(a_t|s_t)$ and a value function $V_\phi(s_t)$ at the same time.

The policy function π_θ is a mapping from state to action distribution. It maps the state s_t to an action distribution $\pi_\theta(a_t|s_t)$, where θ are the policy parameters. The action distribution is defined by the neural network's output, which consists of the mean and variance parameters of a Gaussian distribution. The value function $V_\phi(s_t)$ is a mapping from state to state's value. It estimates the expected return of a state s_t , which is $V_\phi(s_t) = \mathbb{E}\{\sum_{t=t}^{\infty} \gamma^t r_t(s_t, a_t)\}$. ϕ represents the network parameters of the value function.

The value function $V_\phi(s_t)$ can be learned by minimizing the error to the estimated value \hat{R}_t :

$$\phi_{k+1} = \arg \min_{\phi} \sum_{\tau \in \mathcal{D}_k} \sum_{t=0}^T (V_\phi(s_t) - \hat{R}_t)^2 \quad (11)$$

where $\hat{R}_t = r(s_t, a_t) + \gamma V_\phi(s_{t+1})$ is the temporal difference target of $V_\phi(s_t)$ and \mathcal{D}_k is the rollout buffer that stores system transitions $\tau = (s_t, a_t, r_t, s_{t+1})$.

Likewise, the policy function $\pi_\theta(a_t|s_t)$ can be learned by policy gradient methods. $\pi_\theta(a_t|s_t)$ represents the probability distribution of actions a_t under state s_t . i.e. $a_t \sim \pi_\theta(s_t)$. Policy gradient methods estimate the gradient of the policy parameters θ to maximize the following objective:

$$\theta_{k+1} = \arg \max_{\theta} \sum_{\tau \in \mathcal{D}_k} \sum_{t=0}^T \frac{\pi_\theta(a_t | s_t)}{\pi_{\theta_k}(a_t | s_t)} A^{\pi_{\theta_k}}(s_t, a_t) \quad (12)$$

where $\pi_\theta(a_t | s_t)$ and $\pi_{\theta_k}(a_t | s_t)$ are the probabilities of taking action a_t under θ and θ_k (policy parameters used to sample the k th rollout buffer). $A^{\pi_{\theta_k}}(s_t, a_t)$ is an estimate of the *advantage* that can be gained under policy π_{θ_k} from taking action a_t rather than following action distribution $a \sim \pi_{\theta_k}$. $A^{\pi_{\theta_k}}(s_t, a_t)$ is derived based on the trajectory τ and value function V_ϕ [31]. This iterative step maximizes the gained advantage of the updated policy parameter $\theta_k \rightarrow \theta_{k+1}$.

To avoid the policy function from changing too far and causing performance collapse, PPO algorithm[30] adopts a new surrogated policy gradient objective rather than (12):

$$\theta_{k+1} = \arg \max_{\theta} \sum_{\tau \in \mathcal{D}_k} \sum_{t=0}^T \min \left(\frac{\pi_\theta(a_t | s_t)}{\pi_{\theta_k}(a_t | s_t)} A^{\pi_{\theta_k}}(s_t, a_t), g(\epsilon, A^{\pi_{\theta_k}}(s_t, a_t)) \right) \quad (13)$$

where $g(\cdot)$ scales A according to ϵ :

$$g(\epsilon, A) = \begin{cases} (1 + \epsilon)A & A \geq 0 \\ (1 - \epsilon)A & A < 0 \end{cases} \quad (14)$$

This objective makes sure that the updated policy stays close to the original policy. So that the policy won't change too fast to cause performance collapse. For the detailed explanations, please refer to [30].

We can combine the proposed NNSF training framework(Fig. 5) with the PPO RL algorithm. The PPO-based NNSF training approach is summarized in Algorithm 2.

Algorithm 2 PPO-based NNSF Training

```

1: Input: initial NNSF parameters  $\theta_0$ , initial value function
   parameters  $\phi_0$ 
2: for  $k = 0, 1, 2, \dots, N$  do ▷ For  $N$  rollouts
3:   for  $t = 0, 1, 2, \dots, T$  do ▷ For  $T$  timesteps
4:     Get market state  $\hat{s}_t$ , and the market clearing price
        $\lambda_t$ .
5:     Merge market state and market price as the state:
        $s_t = (\hat{s}_t, \lambda_t)$ .
6:     Sample the approximate market clearing result  $p_t$ 
       from the NNSF's output distribution  $p_t \sim \pi_\theta(s_t)$ .
7:     Compute the reward  $r_t$  by market profit (3).
8:     Transit to the next step.
9:     Store the step history to the rollout buffer  $\mathcal{D} \leftarrow$ 
        $(s_t, p_t, r_t, s_{t+1})$ .
10:   end for
11:   Use the rollout buffer to update the function estimates.
12:   Compute advantage estimates,  $\hat{A}_t$  using [31] based on
       the current value function  $V_{\phi_k}$ .
13:   Update the policy  $\pi_\theta$  by maximizing the PPO objective
       of [30].
14:   Fit value function  $V_\phi$  by regression on Value iteration
       of [30].
15:   Empty the rollout buffer  $\mathcal{D}$ .
16: end for

```

Because the neural network structure is not the focus of this paper. In practice, we use common multi-layer perceptron networks that have two hidden layers of 256 nodes as the NNSF network π_θ and value network V_ϕ . All output values are mapped through Tanh activations, which maps the output value from $(-\infty, \infty)$ to $(-1, 1)$. Other training parameters will be detailed in the experiment section.

C. NNSF Refinement for Energy Storage Bidding

In this subsection, we refine the NNSF's output space for ESS bidding.

The original output space of NNSF is the power action p_t , which is a continuous space between -1 and 1 (corresponding to maximum charging and discharging). This output space has difficulties in achieving zero output. Zero output means the ESS's charging and discharging power are both zero. It is a common decision of ESSs, and it helps the ESS to hold the stored energy for more valuable dispatches.

However, it is difficult for neural networks to stay at exactly zero output for a range of input prices. Because neural networks' inside computations are mostly smooth, it can be difficult for neural networks to achieve a full-zero output range.

To assist neural networks to output zero easily, we modify the output space of an NNSF to a 4-dimensional space. It includes the price boundaries for the zero output: $(\lambda_t^d, \lambda_t^c)$, and the power actions beyond the zero output price boundaries: (p_t^d, p_t^c) . The final power action of an NNSF is:

$$p_t = \begin{cases} p_t^d & , \text{ if } \lambda_t \geq \lambda_t^d \text{ (discharging)} \\ -p_t^c & , \text{ else if } \lambda_t \leq \lambda_t^c \text{ (charging)} \\ 0 & , \text{ else} \end{cases} \quad (15)$$

which assures the power action p_t is zero in the range $(\lambda_t^c, \lambda_t^d)$, so that it is easier for neural networks to achieve zero output for a specific price range. The effectiveness of such refinement will be demonstrated in the experiments.

V. PERFORMANCE EVALUATION

In this section, we demonstrate the proposed method's effectiveness in training NNSF and generating HDBs on various market price nodes and different ESS parameters. We also compare it against other existing RL-based bidding methods that use LDBs.

A. Experiment Setup

We consider a real-world ESS in the RT energy market[7]. As an ESS usually has a small portion of the market, we assume it to be a price-taker. It maximizes its profit with HDB bidding(1).

The ESS has ± 1 MW power capacity and different storage capacities ranging from 2MWh to 12MWh. Its charging and discharging efficiency are both 0.95. Its degradation cost λ^{dep} is 10USD/MWh, which means a 1MWh energy cycle has a cost of about 10USD.

The PJM market is a real-world power market that distributes electricity across several states in the Eastern and Midwestern US. Based on the submitted market bids, PJM organizes the buying and selling of electrical energy for 12 \times five-minute intervals of the operating hour. Then, 12 clearing prices and 12 power setpoints are fed back to the bidders as the market clearing result.

The RT market data are collected from the PJM market history. We select five price nodes of the PJM market as the data source, including PJM-RTO (Central Node), DOM (SouthEast), EKPC (SouthWest), COMED (NorthWest), and PSEG (NorthWest). The PJM RT market prices from 2018/4/1-2020/12/25 (1000days) are used to simulate the RT market. The PJM RT market data is split into train and test sets. The first 70% market data are used for training using Algorithm 2 and the last 30% market data are used for testing using Algorithm 1.

In order to effectively arbitrage under high uncertainty, the following observations are provided for the ESS bidder: 1) bid time, denoted as T_t , which is $\sin(T/24), \cos(T/24)$. It is a 2-dimensional sinusoidal encoded time to indicate the time of day. 2) market histories, denoted as h_t . It consists of the angle and amplitude of the first three dimensions in the discrete Fourier Transform of the past 6 hours' RT market price and the past 4 days' DA market price. 3) energy levels, denoted as e_t , which is the SoC of the ESS.

All experiments were run on a PC with an i9-10900X CPU and 128GB memory. The RL algorithms are trained using an NVIDIA 3090 GPU with 24GB memory. We implement the proposed RL algorithm in PyTorch. The detailed hyperparameters are shown in Table I:

TABLE I
RL ALGORITHM HYPERPARAMETERS

Parameter	Value	Parameter	Value
N	10	M	512
Total Steps	3×10^6	Batch Size	256
Action Initial Std	0.6	ϵ_{clip}	0.2
Action Final Std	0.25	γ	0.999
Action Std Decay	$2 \times 10^{-7}/\text{step}$	SoC Violate Penalty P	170 USD
Actor Learning Rate	5×10^{-5}	λ_{\min}	-50 USD
Critic Learning Rate	3×10^{-4}	λ_{\max}	200 USD

B. Benchmark Methods

To verify the effectiveness of the proposed HDB bidding method, it is tested against other RL-based bidders with LDBs.

- 1) Self-Scheduling Bid Learning (Self-Bid)[6]: The Self-Bid method[6] only bids one power quantity p_t , and the power quantity is always accepted by the market.
- 2) Two Pair Bid Learning (Pair-Bid)[22]: The Pair-Bid method[22] bids two price-power pairs. One bid is used for discharging power, and another pair is used for charging power (energy storage only). The power bid p_t is accepted when the market clearing price is higher/lower than the price bid depending on the charging or discharging direction. We consider Pair-Bid to represent the state-of-the-art performance of LDBs.
- 3) Direct HDB Bid Learning (Direct-HDB): Direct-HDB is an upgraded version of Pair-Bid, where N instead of 2 pairs are output by the policy for market bidding. This is the most direct approach to generate HDBs with neural networks, which includes an RL policy with a $2N$ -dimensional output. The first N dimensions are used as price bids, and the next N dimensions are used as power bids. It serves as a baseline to verify the effectiveness of the proposed HDB bidding method.
- 4) HDB Bidding (HDB-Bid): The bidding method proposed in this paper. The NNSF is trained using RL (Algorithm 2), and the HDB generation process (Algorithm 1) is used to generate test results. The NNSF's action space is refined as in Section IV-C
- 5) HDB Bidding without action space refinement (HDB-WOA): The NNSF training and HDB generation process of HDB-WOA is the same as the HDB-Bid method. However, its action space is not refined and is a one-dimensional power output.
- 6) Optimal Bidding (Optimal-Bid): Optimal-Bid is the best possible bidder. It is the upper-bound performance of any actual bidder. In the following context, the bidding results will be scaled based on Optimal-Bid to a percentage representation.

C. General Performance

In this subsection, we compare the general performance of the proposed HDB-Bid bidding method with Self-Bid, Pair-Bid, Direct-HDB, and HDB-WOA. The performance metrics include the training curve, the cumulative test reward and the captured profit ratio. The RL-based ESS bidders are trained for 2.5×10^7 steps in the simulated environment. Each takes

about 2 hours on the mentioned hardware. They are tested on unseen datasets of length 300 days.

1) *Training Curves on the Train Dataset*: The training curves of different RL-based bidding methods is shown in Fig. 6. To ensure a fair comparison between different bid formats, the PPO training algorithm with the same hyperparameter is used for training. Each figure shows the training curves at of specific energy storage capacity. The shown training curves are the average training reward across five price nodes, and the shallow areas in the background are the maximum and minimum training rewards across the five price nodes.

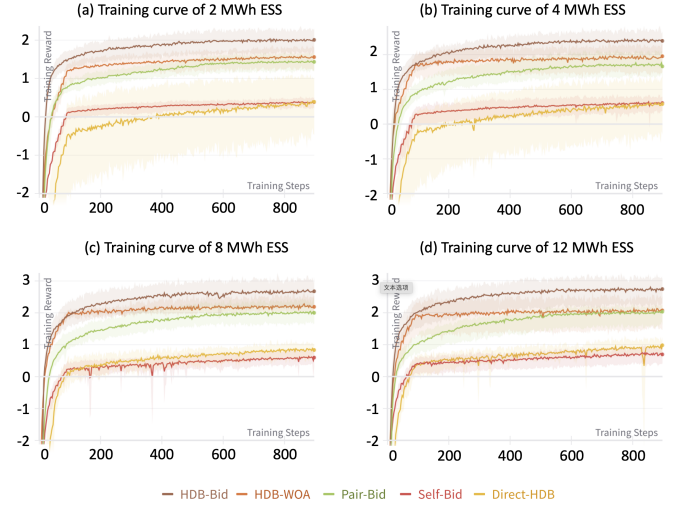


Fig. 6. The training curve of different bidding methods on different energy storage capabilities. The reward values are averaged across five price nodes.

The proposed HDB bidding method outperforms other bidding methods in terms of training speed and performance. It achieves the fastest convergence speed and the highest convergence performance. HDB-WOA has a similar convergence speed in the initial stages. However, the final performance of HDB-WOA is lower because HDB-WOA cannot maintain the NNSF output power at exactly zero, so it is not able to learn power withholding strategies and the bidding performance is affected. The Pair-Bid achieves a training performance similar to that of HDB-WOA but learns in a slower way. The Direct-HDB and Self-Bid exhibit similar training patterns. They have similar training performance in low-capacity cases (2MWh and 4MWh), and Direct HDB has a higher training performance in high-capacity cases (8MWh and 12MWh). Their training performance is mediocre compared with the first three bidding methods.

The different training performances of HDB-based methods demonstrate the effectiveness of the proposed HDB representation and bidding method. Direct-HDB is a direct approach to generating raw HDBs for bidding, but the training performance of Direct-HDB is similar to Self-Bid. Since the Self-Bid is self-dispatch with only one-value power output, this demonstrates that Direct-HDB deteriorates to the bidding performance of the simplest bid format.

By comparing the performance of different bidding formats (HDB, Pair-Bid, and Self-Bid), we can observe that more flex-

ible bidding formats can achieve higher bidding performance. From the perspective of RL, more flexible bidding formats can provide more flexible action spaces (like the price thresholds) and more informative state spaces (like the market price). Both can improve the RL's training performance as long as they can be effectively utilized by the RL algorithms.

2) *Captured Profit Ratios on the Test Dataset*: Next, testing rewards of the comparing methods for different energy storage capacities are listed in Table II and visualized in Fig. 7. All bidding performances are measured against the optimal market bidding result (Optimal Profit).

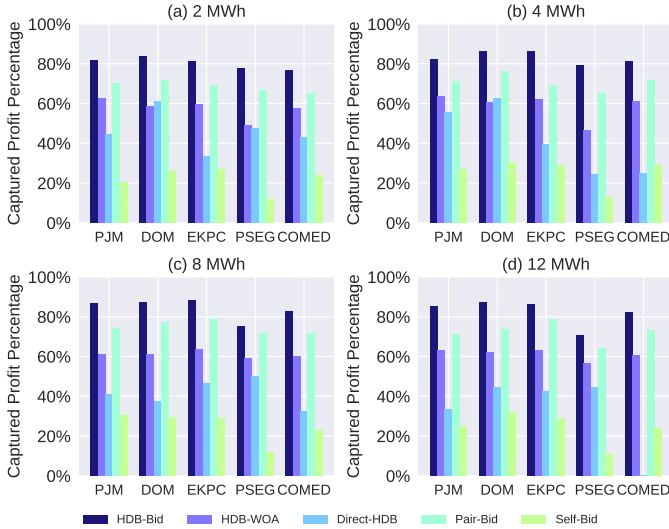


Fig. 7. Captured profit percentage of different bidding methods compared with the optimal market bidding income (which is the 100% levels of the plots)

Fig. 7 shows that HDB-Bid captures a higher percentage of the optimal market profit compared with other low-dimensional bid formats. HDB bidding averagely achieves 15.40% higher profit based on the Pair-Bid bidding method, which is a 10.94% profit boost based on the optimal profit. This shows that higher flexibility in bids enables better learning of bidding strategies and higher income. Self-bid has the lowest bidding reward because it cannot respond to the market price with price bids.

Table II also demonstrates the optimal profit in different price nodes varies a lot. The five price nodes are located in the same market, but their optimal profit in the RT energy market could be doubled from PSED to DOM. Also, the captured profit percentage of RL bidder is higher for high-profit regions (DOM). This shows that the real-time energy market is a location-sensitive market, and the choice of the installed generator can influence the bidding profit by a substantial margin.

In summary, the proposed HDB-Bid method is able to capture 70.84%-88.41% of the optimal profit. It improves the performance by 15.40% based on the low-dimension bids (Pair-Bid) on average. To the best of our knowledge, this is the highest reported profit ratio in the literature captured by RL-based methods for RT energy market bidding.

3) *Cumulative Reward on the Test Dataset*: Fig. 8 shows the cumulative test reward of different bidding methods at the PJM-RTO price node. Due to the limited space, the other four price nodes are not plotted. The horizontal axis is the timestamp, which includes 300 days of unseen data. The vertical axis is the cumulative profit of a 1MW ESS with different energy storage capabilities ranging from 2MWh, 4MWh, 8MWh, to 12MWh.

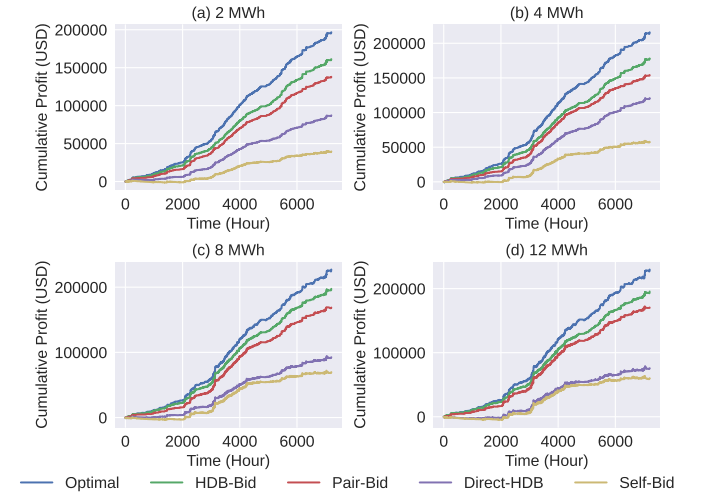


Fig. 8. The cumulative test reward of different bidding methods at the PJM-RTO price node, shown at different energy storage capacities

The HDB-Bid fills the gap from Pair-Bid (previously the most flexible bid) to the optimal bidding income by an average of 43.90%. The gap to the optimal profit for Pair-Bid is 28.31% on average, and for HDB-Bid is 15.88%. The gap is filled by 43.90%, which is a significant boost in terms of bidding profits.

4) *Bid Generation Efficiency*: The efficiency of the HDB generation algorithm (Algorithm 1) is evaluated in this subsection.

Previous RL-based bidding methods generate market LDB by running a neural network forward pass. The neural network's output is the market LDB, such as the one-value power bids[6]. Comparatively, the proposed HDB bidding method generates each market HDB with the HDB generation algorithm (Algorithm 1). For each HDB in Algorithm 1, the neural network is run $M = (\lambda_{\max} - \lambda_{\min}) / \delta\lambda$ times to sample the supply curve. In our case studies, the sample resolution $M = 512$. Then, an HDB extraction process is performed to extract the HDBs.

To evaluate the efficiency of the proposed HDB generation algorithm, we benchmark the runtime of different bid generation methods. The computation time to generate one market bid is computed by averaging over 1000 runs. In Algorithm 1, we also investigate neural network parallelization of batch_size 1 to M in the supply curve sampling process. The run time comparison is shown in Table III

The HDB generation time consists of two parts. The supply curve sampling part and the HDB extraction part. The supply curve sampling process scales linearly w.r.t. the forward pass

TABLE II
BIDDING PERFORMANCE COMPARED WITH OPTIMAL MARKET INCOME IN PERCENTAGE

Node	Capacity	Optimal Profit(USD)	HDB-Bid	HDB-WOA	Direct-HDB	Pair-Bid	Self-Bid
PJM-RTO	2MWh	196695.76	81.94%	62.38%	44.54%	70.37%	20.15%
	4MWh	215900.52	82.46%	63.51%	55.52%	71.04%	26.70%
	8MWh	227115.32	86.99%	61.26%	41.10%	74.10%	30.66%
	12MWh	229876.92	85.08%	63.05%	33.22%	71.23%	24.68%
DOM	2MWh	259200.00	83.51%	58.34%	61.04%	71.65%	25.92%
	4MWh	279523.43	86.16%	60.79%	62.56%	76.28%	30.33%
	8MWh	291301.26	87.11%	60.88%	37.65%	77.10%	29.66%
	12MWh	294945.57	87.44%	62.17%	44.72%	73.67%	31.72%
EKPC	2MWh	210394.50	81.35%	59.78%	33.26%	69.00%	26.87%
	4MWh	227824.98	86.07%	61.85%	39.32%	69.12%	29.10%
	8MWh	237024.77	88.41%	63.73%	46.32%	78.82%	28.95%
	12MWh	239230.74	86.35%	63.18%	42.54%	78.68%	29.09%
PSEG	2MWh	132436.86	77.49%	49.08%	47.49%	66.55%	11.87%
	4MWh	142708.82	79.31%	46.70%	24.19%	64.89%	12.71%
	8MWh	148976.69	75.26%	59.22%	50.10%	67.56%	11.85%
	12MWh	151270.96	70.84%	56.39%	44.28%	64.07%	10.79%
COMED	2MWh	218417.58	76.73%	57.76%	42.79%	64.91%	23.74%
	4MWh	239701.78	81.21%	61.18%	25.04%	71.90%	29.04%
	8MWh	251876.35	82.71%	60.29%	32.39%	71.47%	22.89%
	12MWh	255628.37	82.12%	60.35%	39.74%	73.37%	23.98%
	Variance	47717.22	4.64%	4.46%	10.21%	4.32%	6.92%

TABLE III
GENERATION TIME OF GENERATING A MARKET BID

Method	LDB	HDB batch_size=512	HDB batch_size=16	HDB batch_size=4	HDB batch_size=1	HDB extraction
Time	0.570ms	4.081ms	6.950ms	13.967ms	42.41ms	3.045ms

times of the neural network, ranging from $1ms$ to $40ms$. The HDB extraction part has a constant time of about $3.045ms$.

The results show that parallelization is important for speeding up the HDB generation process. Parallelization of neural network forward can be easily achieved on a single GPU by setting a proper batch size. As a result, even though the proposed approach will consume more computation resources, it still has a similar run time when parallelization is possible.

In summary, the HDB generation has a running time of milliseconds on the mentioned hardware. By neural network forward pass parallelization, the process can reach a running speed of $4.081ms$, which is efficient for hourly power market bidding.

D. Bidding Visualization

In this subsection, we visualize the HDB bidder's bidding history for a more intuitive understanding of its high-dimensional bid decisions.

1) *Bidding process visualization*: Fig. 9 provides a demonstration of a 2-day bidding result on the PJM-RTO price node with different energy storage capacities.

The upper subfigures show the RT energy market prices. The lower subfigures show the SoC histories in black areas and show the market clearing power in red lines. Positive power means discharging, and negative power means charging. We can observe that the RT market price is highly uncertain, and the price peaks are difficult to predict[10, 11].

Overall, the bidder is able to bid strategically. From the perspective of charging (negative power values), the bidder is able to capture the low prices during low-price hours at night. It charges the SoC to proper levels before high-price

times. From the perspective of discharging (positive power values), the bidders are able to precisely capture the high-price peaks and allocate the stored energy among them. During the high-price times, the 2MWh ESS (Fig. 9.a) discharges at the high-price peaks and charges at normal prices to arbitrage. Comparatively, the 12MWh ESS (Fig. 9.d) only discharges during the high-price peaks because it stores enough energy in the low-price hours. Both behaviors are plausible from an ex-ante perspective.

By comparing the power routes and SoC routes of different ESS, we can see that the proposed bidder adapts to the ESS capacity with proper strategies to charge at low market prices and discharge at high market prices.

2) *HDB visualization*: The generated HDBs corresponding to Fig. 9 is demonstrated in Fig. 10. The HDBs for different energy storage capacities are shown in 3D plots. The vertical axis is the discharge power in MW , and the horizontal axes are the bid prices and bid time.

From the perspective of discharging (upper red regions), the bidders usually have a clear price threshold for discharging power. The bidders will choose to discharge above a specific price threshold and choose to be undispached under that threshold. The price threshold is different for ESS with different energy storage capacities. In general, a low-capacity ESS has a more sensitive price threshold that changes with the bidding time. while high-capacity ESS has a more stable price threshold that rarely changes throughout the day. This can be explained by the fact that the change in SoC percentage is deeper for a low-capacity ESS. Therefore, low-capacity ESS changes the price threshold according to the change in energy levels.

From the perspective of staying idle (middle white regions), the bidders are able to withhold energy strategically. The white regions in Fig. 10 denote the time and price that the agents choose to be undispached. ESS with different energy storage capacities will adopt different idle strategies. From the power dispatch results in Fig. 9, we can see that the ESS

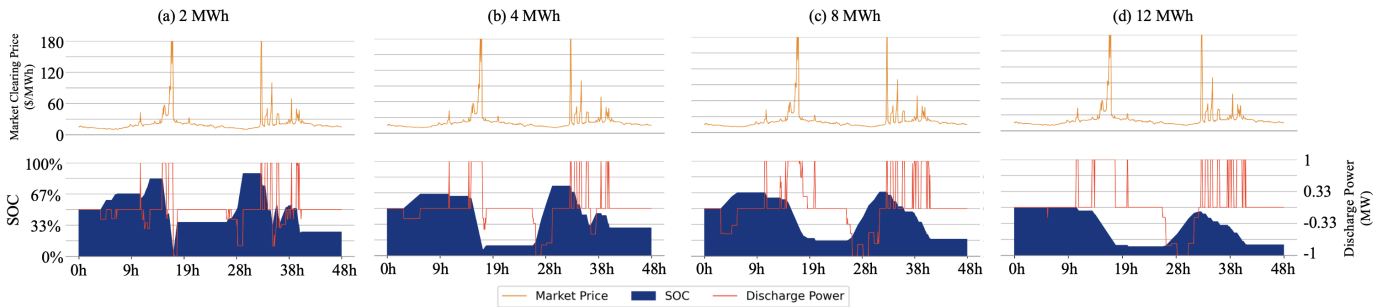


Fig. 9. A sample bidding history of a 1, 2, 4, 8MWh ESS in the PJM-RTO price node. Yellow lines are market clearing prices, red lines are discharge powers of ESS, black areas are the SoC of the ESS.

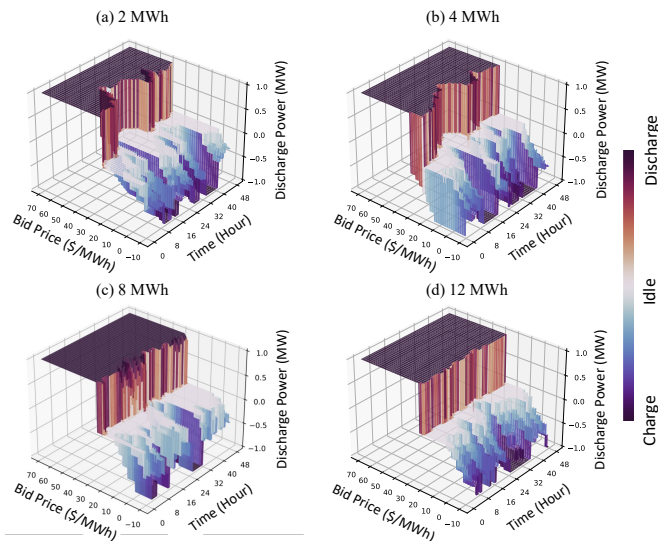


Fig. 10. Demonstration of the historical HDBs corresponding to Fig. 9. The vertical axis is the bidding power. The horizontal axis is the bid price and the time index. One bid corresponds to one hour.

is undischarged for most of the bidding time, rendering the importance of such a strategy.

From the perspective of charging (lower black regions), the bidders utilize the high-dimensionality of HDBs for price-responsive discharge. Bidders will charge different energy for different market prices. The low-capacity bidders are less price-sensitive, as they will conduct charging even if the market price is higher than 20USD/MWh. The high-capacity bidders are more price-sensitive, as they only conduct discharge for prices below 20USD/MWh. This can be explained by their different capability to capture the low prices for charging. Because high-capacity ESS is able to charge large amounts of energy at low prices, they don't need to buy energy when the market price is high. However, low-capacity ESS cannot store much energy during low prices, so they have to buy energy during specific high-price scenarios.

From the above experiments, we can see that HDBs can be effectively generated by the proposed bidder, the HDB's flexibility can be strategically utilized, and the generated HDBs have good interpretability. In the following subsection, we will further discuss the relations between the NNSF and

the HDBs.

E. The Influence of Approximating NNSFs with HDBs

In Section III, we propose an HDB generation algorithm to generate HDBs from NNSFs. The algorithm includes a supply curve sampling process and an HDB extraction process. The supply curve sampling process samples the input-output relationship of the NNSF as a supply curve. It is accurate because the sampling resolution can be arbitrarily increased to meet the precision needs.

However, the HDB extraction process will inevitably cause errors because the extracted 2N-dimensional HDB will lose information from the supply curve. The HDB extraction process includes three steps: the monotone, discretize, and output bid process. (Fig. 3) The monotone step will modify the supply curve if it is not monotonic. The discretize steps will cause approximation errors in extracting 2N-dimensional HDBs from supply curves.

In this subsection, we will further discuss the degree of these two errors and how such approximation errors influence the bidding results. Overall, we found that the monotone step is beneficial to bidding, and the discretize step is minor detrimental.

1) *Comparing the Performance of NNSF and HDB*: The bidding profit of NNSF and HDB are compared in Table IV. They apply the trained NNSF to the training bidding process of Fig. 5 (NNSF), and the HDB generation process of Fig. 1 (HDB). Because the training bidding process directly dispatches the ESS with NNSF, it reflects the direct bidding result of NNSF without HDB generation.

Surprisingly, the HDB achieves higher bidding profit than NNSF. Intuitively, the HDB generation algorithm loses information from the original NNSF. This would cause a performance drop due to the loss of information. However, the test results show that the performance increased by 4.13~9.27%, which is a substantial improvement.

In the following subsections, we find out the reason for such improvement by examining the influence of the monotone and discretize steps.

2) *The Influence of the Monotonize Step of the HDB Generation Algorithm*: In this subsection, we will demonstrate that the Monotonize step in Algorithm 1 is overall beneficial for the bidding results. We will discuss its influence on both the normal price ranges and the extreme price ranges.

TABLE IV
THE CAPTURED PROFIT RATIO OF HDB (APPROXIMATED FROM NNSF) AND NNSF

	PJM-RTO		DOM		EKPC		PSEG		COMED	
	NNSF	HDB	NNSF	HDB	NNSF	HDB	NNSF	HDB	NNSF	HDB
Capacity										
2MWh	77.35%	81.94%	76.20%	83.51%	74.96%	81.35%	70.34%	77.49%	72.19%	76.73%
4MWh	78.01%	82.46%	78.28%	86.16%	80.94%	86.07%	70.04%	79.31%	76.53%	81.21%
8MWh	81.29%	86.99%	79.24%	87.11%	83.07%	88.41%	68.32%	75.26%	78.58%	82.71%
12MWh	80.21%	85.08%	79.30%	87.44%	80.31%	86.35%	62.01%	70.84%	77.56%	82.12%

First, on the normal price ranges (-50USD, 200USD), the learned NNSF $\pi_{\theta}(\hat{s}_t, \lambda_t)$ is monotonic in general. Therefore, the monotonic step will not cause much approximation error for normal price ranges. We will use two metrics to demonstrate the NNSF's monotonicity.

The first metric is the number of monotonic supply curves, which corresponds to the percentage of supply curves that are completely monotonic and do not need to be monotonicized. The second metric is the percentage of supply curve points that need to be changed to achieve total monotonicity. This describes how much the monotonicity assumption is violated from a point-based view and describes how much deviation is introduced in monotonicizing the supply curves.

On the first metric, the percentage of completely monotonic supply curves is 98.24%. This shows that only 1.76% of supply curves are affected by the monotonicize step, and most supply curves are monotonic. On the second metric, the percentage of monotonic supply curve segments is 99.80%. This shows that the monotonicize step will only change 0.2% of the total supply curve segments.

The change of 0.2% change in supply curve segments is relatively negligible from the perspective of the whole NNSF. As a result, the error of the monotonicize step (step b in Algorithm 1) for normal price ranges is small.

Second, on the extreme price ranges (prices beyond the normal price range), the learned NNSF is generally not monotonic. The percentage of completely monotonic supply curves between price 200USD and 500USD is 40.29%, and the percentage of monotonic bidding segments is 62.01%.

The reason for such non-monotonicity is that extreme cases are difficult to train in machine learning. Because extreme prices are rare in the training dataset, they do not have enough training data, so these cases are not fitted enough in the training process. Also, because the extreme cases are numerically ill-conditioned data that deviates from the normal price distribution, they are hard to fit by neural networks.

Therefore, the monotonicize step will change the actions at extreme price ranges. However, the change is beneficial for bidding. The monotonicize step will overwrite the action of the extreme price ranges with the action of the normal price ranges, which involves full discharge power for extremely high prices and full charge power for low prices. It helps the bidding agent to achieve plausible actions for extreme prices.

As a result, the monotonicize step is beneficial overall for bidding performance. The average captured profit percentage of the monotonicized supply curve is 82.59%, which is higher than the HDB-Bid (82.43%) and the NNSF (76.24%). In the following context, we will use $N=\infty$ to denote the monotonicized supply curve, which is a discretized supply curve with

infinite resolution.

3) *The Influence of the Discretize Step of the HDB Generation Algorithm* : In this subsection, we will show that the discretize step in Algorithm 1 will negatively impact the bidding performance, but the influence is minor because the HDB is high-dimensional and flexible. We will compare the performances of the monotonicized supply curve with different dimensions of HDBs. Then, we will measure the discretization errors from the monotonicized supply curve to HDB.

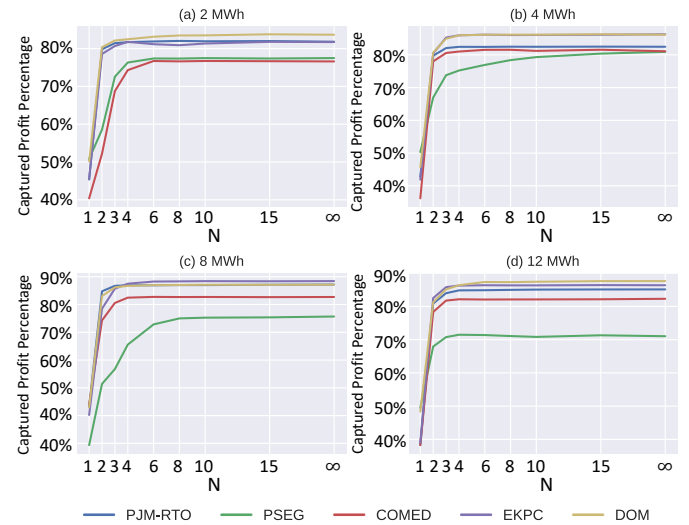


Fig. 11. The captured profit ratio of HDBs with different dimensions. The horizontal axis is N, which is the degree of freedom of the bidding pairs.

The bidding performance of HDBs with different dimensions is shown in Fig. 11. The bidding performance is shown in the captured profit ratios and grouped by SoC values.

In general, a higher HDB dimension (a higher N) achieves a better bidding performance. The $N=1$ case has the lowest captured profit because its flexibility is the lowest. The average capture profit percentage of $N=1$ across all experiments is 43.10%. From $N=2$ to $N=6$, the captured profit percentage of HDBs gradually increases. The average captured profit percentage is 74.91%($N=2$), 79.78%($N=3$), 81.37%($N=4$) and 82.16%($N=6$). For $N \geq 6$, the profit is mostly saturated, and the performance increases slowly. The average captured profit percentage is 82.34%($N=8$), 82.43%($N=10$), 82.58%($N=15$). Finally, the monotonic supply curve ($N=\infty$) has a captured profit ratio of 82.59%.

$N=10$ is the most common HDB format, and its performance is close to $N=\infty$ (no discretization). The gap from $N=10$ to $N=\infty$ is 0.16% profit percentage, which means the common HDBs can capture sufficient profits for the bidding.

$N=2$ corresponds to the Pair-Bid bidding format[22]. Its performance gap to $N=10$ is 7.52%, and its performance gap to $N=\infty$ is 7.68%. This shows that the Pair-Bid format could lose a considerable amount of profit in real-world bidding.

Additionally, we quantify the errors of the discretize step by comparing the market clearing power of HDB-Bid ($N=10$) and the monotonized supply curve ($N=\infty$). We measure the mean absolute error (MAE) of market clearing power from monotonic supply curves to HDBs. The MAE is 0.0103 (with full power as ± 1), which is 1.03% of the maximum power.

Overall, the discretize step will introduce approximation errors to the bidding process, but the approximation error and the performance drop of most market's HDBs is minor for real-world bidding.

F. Discussions and Further Applications

From the above experiments, we can see that using NNSF for training and generating HDBs for real-world bidding can produce high-performance bidding results. Though the framework includes various approximations, including the monotonize and discretize steps in Section III-C, and the market clearing power approximation in Section IV-A, the bidding results are satisfactory.

This phenomenon relates to the problem's characteristics. On the one hand, the discretize step and the market clearing power approximation are accurate because the HDB is a high-dimensional bid, and it can represent the NNSF with high precision. On the other hand, the monotonize step is accurate because the bidder is profit-seeking, and it will tend to bid more power for a higher market clearing price in normal price ranges, and it is originally monotonic in most cases. As a result, the proposed training process is accurate for training NNSFs and generating HDBs.

The proposed framework provides a new way for RL-based HDB bidding: we can learn an NNSF first and use HDBs to approximate it. So that HDBs can be learned and generated effectively.

Regarding the RL problem's structure, the proposed framework transforms the market price λ_t from an unknown input to a known input of the neural network agent. Which makes the bidding problem a simpler task for RL algorithms to learn.

In the future, the proposed NNSF process can be applied to other HDB bidding scenarios, such as the Day-Ahead energy market, the regulation market, the reserve market, etc.

VI. CONCLUSION

This paper proposes a bidding framework that effectively utilizes HDBs for the first time in RL-based power market bidding methods. Though the HDB is the most common market bidding format in the form of N price-power pairs, past RL-based methods have failed to fully utilize the HDB for power market bidding due to its high dimensionality. The loss of flexibility in current RL bidding methods could greatly limit bidding profits and make it difficult to tackle the rising uncertainties brought by renewable energy generations. To tackle the above challenges, we propose a framework that

is suitable for RL-based methods with HDB bidding. First, we employ a special kind of neural network called NNSF to construct a strategic mapping from market clearing price to bidding power. Second, we propose a generation framework to extract HDBs from the input-output relation of NNSF. Then, we propose an approximation of the generation framework and compose a new training framework, which is compatible with most state-of-the-art RL algorithms. Finally, a PPO-based RL algorithm is employed to train an HDB bidding policy for an ESS in the RT energy market. Experiment results show that the proposed algorithm is able to efficiently leverage the bid flexibility of HDBs and generate strategic HDB bidding pairs. The proposed algorithm can improve the bidding performance based on state-of-the-art RL methods by an average of 15.40% and reaches 70.84%~88.41% optimal market profit, which is the highest reported profit ratio in the literature captured by RL-based methods for RT energy market bidding. The future work includes empowering a larger number of RL-based power market bidding methods with the flexibility of HDBs using the proposed bidding framework.

REFERENCES

- [1] T. Kempitaya, S. Sierla, D. De Silva, M. Yli-Ojanperä, D. Alahakoon, V. Vyatkin, An Artificial Intelligence framework for bidding optimization with uncertainty in multiple frequency reserve markets, *Applied Energy* 280 (2020) 115918. doi:10.1016/j.apenergy.2020.115918.
- [2] S. Cevik, K. Ninomiya, Chasing the sun and catching the wind: Energy transition and electricity prices in Europe, *Journal of Economics and Finance* (Jun. 2023). doi:10.1007/s12197-023-09626-x.
- [3] A. Rai, O. Nunn, On the impact of increasing penetration of variable renewables on electricity spot price extremes in Australia, *Economic Analysis and Policy* 67 (2020) 67–86. doi:10.1016/j.eap.2020.06.001.
- [4] International Renewable Energy Agency, Renewable capacity statistics 2023, <https://www.irena.org/Publications/2023/Mar/Renewable-capacity-statistics-2023> (Mar. 2023).
- [5] J. Bian, Y. Song, C. Ding, J. Cheng, S. Li, G. Li, Optimal Bidding Strategy for PV and BESSs in Joint Energy and Frequency Regulation Markets Considering Carbon Reduction Benefits, *Journal of Modern Power Systems and Clean Energy* 12 (2) (2024) 427–439. doi:10.35833/MPCE.2023.000707.
- [6] X. Wei, Y. Xiang, J. Li, X. Zhang, Self-Dispatch of Wind-Storage Integrated System: A Deep Reinforcement Learning Approach, *IEEE Transactions on Sustainable Energy* 13 (3) (2022) 1861–1864. doi:10.1109/TSTE.2022.3156426.
- [7] Day-Ahead, R.-T. M. Operations, PJM manual 11: Energy and ancillary services market operations revision: 123 (Oct. 2022).
- [8] CAISO, Real-Time Market Activities, Version No. 11.2, Procedure No. 2210 <https://www.caiso.com/documents/2210.pdf> (Feb. 2023).

- [9] A. E. M. Operator, Integrating Energy Storage Systems - High Level Design (Jul. 2022).
- [10] Z. Zhang, M. Wu, Predicting Real-Time Locational Marginal Prices: A GAN-Based Approach, *IEEE Transactions on Power Systems* 37 (2) (2022) 1286–1296. doi:10.1109/TPWRS.2021.3106263.
- [11] H. Yang, K. R. Schell, QCAE: A quadruple branch CNN autoencoder for real-time electricity price forecasting, *International Journal of Electrical Power & Energy Systems* 141 (2022) 108092. doi:10.1016/j.ijepes.2022.108092.
- [12] J. Wang, J. Xu, J. Wang, D. Ke, L. Yao, Y. Zhou, S. Liao, Two-stage distributionally robust offering and pricing strategy for a price-maker virtual power plant, *Applied Energy* 363 (2024) 123005. doi:10.1016/j.apenergy.2024.123005.
- [13] R. Herding, E. Ross, W. R. Jones, V. M. Charitopoulos, L. G. Papageorgiou, Stochastic programming approach for optimal day-ahead market bidding curves of a microgrid, *Applied Energy* 336 (2023) 120847. doi:10.1016/j.apenergy.2023.120847.
- [14] A. Najafi-Ghalelou, M. Khorasany, R. Razzaghi, Maximizing social welfare of prosumers in neighborhood battery-enabled distribution networks, *Applied Energy* 359 (2024) 122622. doi:10.1016/j.apenergy.2024.122622.
- [15] M. Karasavvidis, A. Stratis, D. Papadaskalopoulos, G. Strbac, Optimal Offering of Energy Storage in UK Day-ahead Energy and Frequency Response Markets, *Journal of Modern Power Systems and Clean Energy* 12 (2) (2024) 415–426. doi:10.35833/MPCE.2023.000737.
- [16] J. Jeong, S. W. Kim, H. Kim, Deep Reinforcement Learning Based Real-Time Renewable Energy Bidding With Battery Control, *IEEE Transactions on Energy Markets, Policy and Regulation* 1 (2) (2023) 85–96. doi:10.1109/TEMPR.2023.3258409.
- [17] J. Li, C. Wang, Y. Zhang, H. Wang, Temporal-Aware Deep Reinforcement Learning for Energy Storage Bidding in Energy and Contingency Reserve Markets, *IEEE Transactions on Energy Markets, Policy and Regulation* (2024) 1–15doi:10.1109/TEMPR.2024.3372656.
- [18] M. Anwar, C. Wang, F. De Nijs, H. Wang, Proximal Policy Optimization Based Reinforcement Learning for Joint Bidding in Energy and Frequency Regulation Markets, in: 2022 IEEE Power & Energy Society General Meeting (PESGM), IEEE, Denver, CO, USA, 2022, pp. 1–5. doi:10.1109/PESGM48719.2022.9917082.
- [19] D. Esmaeili Aliabadi, K. Chan, The emerging threat of artificial intelligence on competition in liberalized electricity markets: A deep Q-network approach, *Applied Energy* 325 (2022) 119813. doi:10.1016/j.apenergy.2022.119813.
- [20] T. Wang, Z. Y. Dong, Adaptive personalized federated reinforcement learning for multiple-ESS optimal market dispatch strategy with electric vehicles and photovoltaic power generations, *Applied Energy* 365 (2024) 123107. doi:10.1016/j.apenergy.2024.123107.
- [21] Y. Du, F. Li, H. Zandi, Y. Xue, Approximating Nash Equilibrium in Day-ahead Electricity Market Bidding with Multi-agent Deep Reinforcement Learning, *Journal of Modern Power Systems and Clean Energy* 9 (3) (2021) 534–544. doi:10.35833/MPCE.2020.000502.
- [22] Y. Tao, J. Qiu, S. Lai, Deep Reinforcement Learning Based Bidding Strategy for EVAs in Local Energy Market Considering Information Asymmetry, *IEEE Transactions on Industrial Informatics* 18 (6) (2022) 3831–3842. doi:10.1109/TII.2021.3116275.
- [23] K. Ren, J. Liu, X. Liu, Y. Nie, Reinforcement Learning-Based Bi-Level strategic bidding model of Gas-fired unit in integrated electricity and natural gas markets preventing market manipulation, *Applied Energy* 336 (2023) 120813. doi:10.1016/j.apenergy.2023.120813.
- [24] Q. Jia, Y. Li, Z. Yan, C. Xu, S. Chen, A Reinforcement-learning-based Bidding Strategy for Power Suppliers with Limited Information, *Journal of Modern Power Systems and Clean Energy* 10 (4) (2022) 1032–1039. doi:10.35833/MPCE.2020.000495.
- [25] Y. Liang, C. Guo, Z. Ding, H. Hua, Agent-Based Modeling in Electricity Market Using Deep Deterministic Policy Gradient Algorithm, *IEEE Transactions on Power Systems* 35 (6) (2020) 4180–4192. doi:10.1109/TPWRS.2020.2999536.
- [26] B. S. Pedasingu, E. Subramanian, Y. Bichpuriya, V. Sarangan, N. Mahilong, Bidding Strategy for Two-Sided Electricity Markets, in: Proceedings of the 7th ACM International Conference on Systems for Energy-Efficient Buildings, Cities, and Transportation, BuildSys '20, Association for Computing Machinery, New York, NY, USA, 2020, pp. 110–119. doi:10.1145/3408308.3427976.
- [27] J. Wang, J. Wu, Y. Che, Agent and system dynamics-based hybrid modeling and simulation for multilateral bidding in electricity market, *Energy* 180 (2019) 444–456. doi:10.1016/j.energy.2019.04.180.
- [28] M. Mallaki, M. S. Naderi, M. Abedi, S. D. Manshadi, G. B. Gharehpetian, Strategic Bidding in Distribution Network Electricity Market Focusing on Competition Modeling and Uncertainties, *Journal of Modern Power Systems and Clean Energy* 9 (3) (2021) 561–572. doi:10.35833/MPCE.2019.000177.
- [29] B. Xu, M. Korpas, A. Botterud, Operational Valuation of Energy Storage under Multi-stage Price Uncertainties, in: 2020 59th IEEE Conference on Decision and Control (CDC), IEEE, Jeju, Korea (South), 2020, pp. 55–60. doi:10.1109/CDC42340.2020.9304081.
- [30] J. Schulman, F. Wolski, P. Dhariwal, A. Radford, O. Klimov, Proximal Policy Optimization Algorithms (Aug. 2017). arXiv:1707.06347, doi:10.48550/arXiv.1707.06347.
- [31] J. Schulman, P. Moritz, S. Levine, M. Jordan, P. Abbeel, High-Dimensional Continuous Control Using Generalized Advantage Estimation (Oct. 2018). arXiv:1506.02438, doi:10.48550/arXiv.1506.02438.